International Journal of Advanced Trends in Computer Applications
www.ijatca.com

Slip Effects on Convective Flow Driven by Two Stretchable Rotating Disks in an Orthotropic Porous Medium

[1]K. Gowthami, [2]Hari Prasad. P, [3]Mallikarjuna. B
[1] Research Scholar, Department of Mathematics,
Koneru Lakshmaiah Education Foundation, Guntur-522502 (India)
[2] Assistant Professor, Department of Mathematics,
Koneru Lakshmaiah Education Foundation, Guntur-522502 (India)
[3] Department of Mathematics, BMS College of Engineering,
Bangalore – 560019 (India)
[1]kambampatigowthami@gmail.com, [2]hariprasad_cse@kluniversity.in, [3]mallikarjuna.jntua@gmail.com

Abstract: *In this paper, an impact of slip on heat flow between stretchable disks in an orthotropic porous medium has been investigated. Stretchable Disks are maintained with uniform constant angular velocities. A set of equations are solved numerically and the results are discussed with the aid of graphs. The impact of the fluid temperature and velocity profiles, for changing values of the governing parameters are explained with graphical representation and table values. It is found that the temperature profiles are decreased as Darcy number increases. Temperature increases with the increased value of stretching parameters. The physical aspects of the problem are highlighted and discussed.*

Keywords: Orthotropic Porous Media, Slip Effects, Rotating Stretchable Disks.

I. INTRODUCTION

Over the past five decades many scientists focused their attention on the study of convective flow with slip effects. This concept has various engineering applications like polymer extrusion, glass fiber, paper production, malleability of plastic, ductility of wires etc. Technical applications like internal cavities and polishing of artificial heart valves utilize those fluids which exhibit boundary slip. Biswal et al. (2007) investigated on gaseous slip effects on free convective flow due to the effect of entrance region in vertical micro-channel. Bhattacharya et al. (2011) discussed impact of slip on heat transport from stagnation point flow from a vertical shrinking sheet. Srinivasacharya (2012) investigated the effect of ion slip and Hall on free and forced convective flow of couple stress fluid in a channel. Slip and transpiration thermal radiation effects on MHD flow from an exponentially vertical stretching sheet has been investigated by Mukhopadhyay (2013). Hayat et al. (2014) studied cross diffusion, slip and Joule heating effects in free and forced convection peristaltic flow of a nanofluid. Noor et al. (2015) presented combined free and forced convection flow of a micropolar fluid past a vertical stretching surface with nanofluid and slip effects. Brownian effect and thermophoresis effects on convective flow of Al_2O_3 nanofluid in an inclined enclosure has been presented by Meissam et al. (2016). Umar Khan et al. (2017) studied slip and heat transfer effects on carbon nanotubes suspended nanofluid flow in a non-uniform channel. Yahaya et al.(2018) investigated on convective heat transfer flow past a nonlinear stretching porous surface with slip and convective boundary effects. Iskander et al. (2019) investigated on Navier slip and convective boundary conditions on MHD double diffusive flow of nanofluid past a static wedge.

The flow over the rotating disks is one of the topics studied by many researchers from the classic fluid mechanics. This concept has various uses in engineering and industrial applications like lubrication, oceanography, MHD pumps, MHD power generators, petroleum industries and certain electronic devices with rotating parts etc. Dileep and Rashmi (2010) investigated magnetohydrodynamic Darcy flow of a viscous fluid between rotating channel with hall current

effect. Anoj kumar and Bhadauria (2011) studied non-linear convective Darcy flow of a non-Newtonian viscoelastic fluid in a rotating porous layer. Sheikholeslami et al. (2012) investigated convective heat transfer flow of "cu-water" nanofluid in a channel with one wall is stretching sheet and other is porous surface in a rotating system. Dhananjay et al. (2013) studied numerically on convective instability in a rotating nanofluid layer. Mustafa (2014) investigated flow and heat transfer of nanofluid containing various nanoparticle volume fractions of Ag, Cu, Al_2O_3, Ag, TiO_2 and CuO driven by a rotating disk. Ahmed and Turan (2015) developed model of heat and mass transfer flow in a porous channel in a rotating system. Mallikarjuna et al. (2016) studied on Non - Darcy buoyancy driven flow from a rotating cone with transpiration and thermophoresis effects. Hayat et al. (2017) discussed Cattaneo – Christov heat flux model on driven flow between two rotating stretchable disks. Mallikarjuna et al. (2017) studied heat and mass transfer flow along a rotating cone in porous medium with non - linear convection and thermophoresis effects. To the best of author knowledge with availability of literature no one has studied on heat transfer flow between two rotating stretchable disks in an orthotropic porous medium which the authors aimed to investigated.

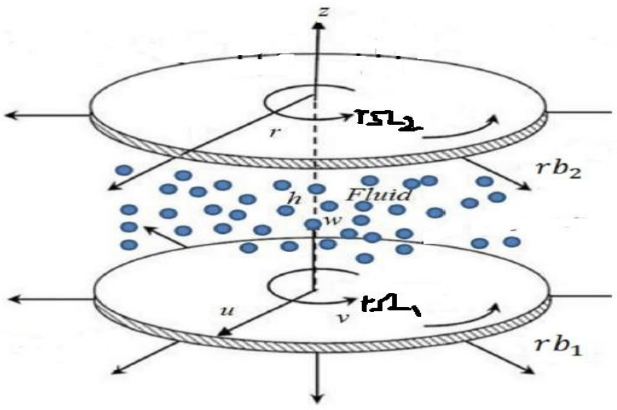

Figure 1: Geometry of the problem

Consider two dimensional viscous incompressible1 fluid between rotating disks as shown in fig-1. The lower disk is placed at z=0 and upper disk is placed at z=h. The lower and upper disks are rotating with different angular velocities Ω_1 and Ω_2 respectively. Both the disks are assumed to be stretched in radial direction for various stretching rates b_1 and b_2 respectively. The lower and upper disks are maintained with different uniform constant temperature T_0 and T_1 respectively. The total system is embedded in orthotropic porous medium. With the above assumption the governing equation in polar coordinates are (Anwar Beg (2017)):

II. FLOW BETWEEN ROTATING DISKS MODEL

$$\left(\frac{\partial}{\partial r}+\frac{1}{r}\right)U+\frac{\partial(W)}{\partial z}=0 \tag{1}$$

$$\left(U\frac{\partial}{\partial r}+W\frac{\partial}{\partial z}\right)U-\frac{V^2}{r}=\frac{-1}{\rho}\frac{\partial p}{\partial r}+\upsilon\left(\frac{\partial^2}{\partial r^2}+\frac{1}{r}\frac{\partial}{\partial r}+\frac{\partial^2}{\partial z^2}-\frac{1}{r^2}\right)U-\frac{\upsilon}{K_r}U \tag{2}$$

$$\left(U\frac{\partial}{\partial r}+W\frac{\partial}{\partial z}+\frac{U}{r}\right)V=\upsilon\left(\frac{\partial^2}{\partial r^2}+\frac{1}{r}\frac{\partial}{\partial r}+\frac{\partial^2}{\partial z^2}-\frac{1}{r^2}\right)V-\frac{\upsilon}{K_\theta}V \tag{3}$$

$$\left(U\frac{\partial}{\partial r}+W\frac{\partial}{\partial z}\right)W=\frac{-1}{\rho}\frac{\partial p}{\partial z}+\upsilon\left(\frac{\partial^2}{\partial r^2}+\frac{1}{r}\frac{\partial}{\partial r}+\frac{\partial^2}{\partial z^2}\right)W-\frac{\upsilon}{K_z}W \tag{4}$$

$$\left(\left(U\frac{\partial}{\partial r}+w\frac{\partial}{\partial z}\right)-\alpha\left(\frac{\partial^2}{\partial r^2}+\frac{1}{r}\frac{\partial}{\partial r}+\frac{\partial^2}{\partial z^2}\right)\right)T=0 \tag{5}$$

Associated boundary conditions are

$$U=s_1\frac{\partial U}{\partial z}+rb_1, V=s_2\frac{\partial V}{\partial z}+r\Omega_1, W=0, T=t_1\frac{\partial T}{\partial z}+T_0 \text{ at } z=0$$

$$U=-s_1\frac{\partial U}{\partial z}+rb_2, V=-s_2\frac{\partial V}{\partial z}+r\Omega_2, W=0, T=-t_1\frac{\partial T}{\partial z}+T_1 \text{ at } z=d \tag{6}$$

Where K_r K_z and K_θ are permeabilities in r, z and θ directions respectively, velocity components $[U,V,W]$ are in $[r,\theta,z]$ directions respectively, υ is the kinematic 1viscosity, ρ is density, , and α is the thermal conductivity of fluid.

In order to non-dimensionalize the eqns. (1) – (6), Introducing the following transformations

$$U = r\Omega_1 f'(\eta), V = r\Omega_1 g(\eta), W = -2\Omega_1 h f(\eta),$$
$$\eta = \frac{z}{h}, \Theta = \frac{T - T_1}{T_0 - T_1}, p = \rho\Omega_1 \upsilon\left(P(\eta) + \frac{r^2}{2h^2}\varepsilon \right) \quad (7)$$

Using (7), eqns. (1) – (6) becomes

$$f''' - \frac{1}{\mathrm{Re}}\left((f')^2 - 2ff'' - g^2 \right) - \varepsilon - \frac{1}{K_1} f' = 0 \quad (8)$$

$$g'' - \frac{2}{\mathrm{Re}}\left(f'g - fg' \right) - \frac{1}{K_2} g = 0 \quad (9)$$

$$P' + \mathrm{Re}\, ff' + 2f'' - \frac{2}{K_3} f = 0 \quad (10)$$

$$\Theta'' + 2\,\mathrm{Re}\,\mathrm{Pr}\, f\Theta' = 0 \quad (11)$$

with the boundary conditions given as

$$f(0) = 0,\ f'(0) = R_1 + S_1 f''(0), g(0) = 1 + S_2 g'(0), \Theta(0) = 1 + t_s \Theta'(0)$$
$$f(1) = 0,\ f'(1) = R_2 - S_1 f''(1), g(1) = \Omega - S_2 g'(0), \Theta(1) = -t_s \Theta'(1) \quad (12)$$

Where $\mathrm{Re} = \frac{\Omega_1 h^2}{\upsilon}$ is1 the Reynold's number, $\mathrm{Pr} = \frac{\upsilon}{\alpha}$ is the 1Prandtl's number, $K_1 = \frac{K_r}{h^2}$ Darcy number along r-direction, $K_2 = \frac{K_\theta}{h^2}$ Darcy number along θ-direction, $K_3 = \frac{K_z}{h^2}$ Darcy number along z-direction, $\Omega = \frac{\Omega_2}{\Omega_1}$ rotation parameter, $R_1 = \frac{b_1}{\Omega_1}$, $R_2 = \frac{b_2}{\Omega_2}$ are scaled stretching parameters, $S_1 = \frac{s_1}{h}, S_2 = \frac{s_2}{h}$ are velocity slip parameters and $t_s = \frac{t_1}{h}$ is the thermal slip parameter

The skin friction coefficients at both disks are:

$$\tau_1 = \frac{\tau_w|_{z=0}}{\rho\left(r\Omega_1\right)^2} \Rightarrow \text{At lower disk } \tau_1 = \frac{\left(\left(f''(0) \right)^2 + \left(g'(0) \right)^2 \right)^{1/2}}{\mathrm{Re}_r},$$

$$\tau_2 = \frac{\tau_w|_{z=h}}{\rho\left(r\Omega_2\right)^2} \Rightarrow \text{At upper disk } \tau_1 = \frac{\left(\left(f''(1) \right)^2 + \left(g'(1) \right)^2 \right)^{1/2}}{\mathrm{Re}_r} \quad (13)$$

Rate of heat transfers (Nusselt numbers) at both disks are:

Table 1: Comparison of $g'(0)$ and $f''(0)$ for changes of Ω when R_1=0, R_2=0 and in the absence of porous medium for Re=1

Ω	**K.Stewartson (1953)**		**M. Imtiaz et.al (2016)**		**Present results**	
	$-g'(0)$	$f''(0)$	$-g'(0)$	$f''(0)$	$-g'(0)$	$f''(0)$
-1	2.00095	0.06666	2.00095	0.06666	2.00095376	0.06666263
-0.3	1.30442	0.10395	1.30442	0.10395	1.30442628	0.10395043
0.5	0.50261	0.06663	0.50261	0.06663	0.50261755	0.06663394

III. RESULTS AND DISCUSSION

The effect of the parameter k_2 and $k_1$on the radial is illustrated in the fig 2 & 3 and noticed that the radial velocity increases with the increase of $k_1$near the stretchable disks i.e. η<0.23 and η>0.8 and effect is decreasing within the middle portion of the developed flow i.e. 0.23< η<0.8 where as, it increases with increase in k_2. Increasing permeability decreases the concentration of solid particles in the regime, i.e., increases the presence of voids. This serves to suppress thermal conduction heat transfer in the regime and acts to reduce temperatures. There will, however, be a corresponding increase in heat transferred to the cone surface with increasing values of r-direcion Darcy number. The influence of Darcy number on the temperature field is less prominent than on the radial velocity. Fig.3 noticed that temperature profiles are decreased as $k_1 and\ k_2$ increases and also observed that temperature profiles in the range of η<0.5 are decreased and opposite results are reported in $\eta > 0.5$.

The effect of one of the velocity slip parameters S_1 on the radial velocity is depicted in the fig.4. It is observed that fluid radial velocity decreases with the increase of S_1 in η<0.23 and η>0.8 increases within the middle developed flow region i.e. 0.23< η<0.8. Fig.5 shows that 1the variation of temperature for various values of S_1. The temperature profiles increases in η<0.5 and then decreases in η>0.5 for larger values of S_1.

Fig.6 and 7 show the radial velocity and temperature profiles for larger values of S_2. Noticed from figs.6&7 that there is no much impact of S_2 on radial velocity and temperature results. It is also observed from the graphs that the radial velocity decreases η<0.5 and then increases for η>0.5 and it is parabolic behavior in nature. Temperature profile for thermal slip parameter t_s is presented in fig.8. It is seen that temperature profile decreases in η<0.5 and then increases in η>0.5 for larger values of t_s.

Table 2 depicts the effects of Darcy numbers on skin friction $(\tau_1 \text{ and } \tau_2)$ coefficients and Nusselt number $(Nu_1 \text{ and } Nu_2)$ values at both disks. With increased values of $k_1$and k_2 the skin friction $(\tau_1 \text{ and } \tau_2)$ coefficient at both disks were decreased where as Nusselt number $(Nu_1 \text{ and } Nu_2)$ results are reported reversely that is increased at both disks. Table 3 predicts velocity and thermal slip parameters on skin friction $(\tau_1 \text{ and } \tau_2)$ coefficients and Nusselt numbers $(Nu_1 \text{ and } Nu_2)$ at both stretchable disks. When S_1increases, skin friction $(\tau_1 \text{ and } \tau_2)$ coefficient and Nusselt number $(Nu_1 \text{ and } Nu_2)$ values are decreased at disks. Increasing S_2 leads to retards skin friction $(\tau_1 \text{ and } \tau_2)$ coefficient at both disks and Nusselt number $(Nu_1 \text{ and } Nu_2)$ reported opposite results at different disks. With the increased values of thermal slip parameter t_s causes to depreciate Nusselt number $(Nu_1 \text{ and } Nu_2)$ at both disks but variation of skin friction $(\tau_1 \text{ and } \tau_2)$ coefficient almost remains constant at two disks.

IV. CONCLUSION

An analysis has been investigated on convective hydrodynamic flow between two stretchable disks. Flow in orthotropic porous medium is described by Darcy's law. Shooting technique is employed to compute the solutions of non-dimentionalized governing equations. Comparison results with existing results are reported to validate the present results. Variation of governing parameters on fluid temperature and fluid velocity as well as skin friction $(\tau_1 \text{ and } \tau_2)$ coefficients and Nusselt number results are discussed with the aid of graphs.

Conflict of Interest

Both the authors have equal contribution in this work and it is declared that there is no conflict of interest for this publication.

Acknowledgment

The authors express their sincere gratitude to the referees for their valuable suggestions towards the improvement of the paper.

References

[1] Ahmed, A., & Turan, A. (2015). *Heat and Mass Transfer*, 51, 497-505.

[2] Anwar Beg, O., Prasad, V.R., Vasu B., & Gorla, R.S.R. (2017). *Journal of Brazilian Society for Mechanical Science and Engineering*, 39(6), 2035-2054.

[3] Biswa.Ll.,.Som,S.K., & Chakraborty, S. (2007). *International Journal of Heat and Mass Transfer*, 50, 1248-1254.

[4] Bhattacharya, K., Mukhopadhyay, S., & Layek, G.C. (2011). *International Journal of Heat and Mass Transfer* 54, 308-313.

[5] Dhananjay, Y., Bhargava, R., & .Agarwal, G.S. (2013). *International Journal of Heat and Mass Transfer*, 63, 313-322.

[6] Hayat, T., Abbasi, F.M., Al – Yami M., & Monaquel, S. (2014). *Journal of Molecular Liquids*, 194, 93-99.

[7] Hayat, T ., Haider, F., Muhammad, T., & Alsaedi, A. (2017). *International Journal of heat and Mass Transfer*, 112, 248-254.

[8] Imtiaz, M., Hayat, M., Alsaedi, A., Ahmad , B. (2016). *International journal of heat and mass transfer*, 101, 948-957,

[9] Iskander, T., Hamadneh, N.N., & Khan, W.A. (2019). *Arabian Journal for science and Engineering*, 44, 1255-1267.

[10] kumar , A., & Bhadauria, B.S. (2011). Transport in Porous Media, 87, 229-250.

[11] Mallikarjuna, B.,.Rashad, A.M., Ahmed Kadhim Hussein, & Hariprasad Raju, S. (2016). *Arab J SciEng*, 41, 4691 – 4700.

[12] Mallikarjuna, B., Rashidi, M. M., & Hariprasad Raju, S. (2017). *Thermal Sciences*, 21, 6B, 2781 – 2793.

[13] Mallikarjuna, B .,.Rashad, A.M., Ali.J., Chamkha & Hariprasad Raju, S. (2016). *Afrika Mathematika*, 27, 645-665,

[14] Meissam, E., Babak, M., Arash, K. P., & Hossein Ali. (2016). *International Journal of Thermal Sciences*, 105, 137 – 158.

[15] Mukhopadhyay, S. (2013). *An Shams Engineering Journal* 4, 485-491.

[16] Mustafa, T. (2014). *Computers & Fluids*, 94, 139-146.

[17] Noor, N.F.M., Ul Haq, R., & Nadeem, S. (2015). *Meccanica*, 50(8), 2007-202.

[18] Sheikholeslami, M., Ashorynejad, H.R., Domairry, G., & Hashim, I., *Journal of Applied Mathematics*, Article: 421320, 18 pages, (2012).
[19] Singh Ch. D., &. Rashmi, A., (2010).*Chem. Engg. Comm.* 197, 830-845.
[20] Srinivasacharya, D., & Kakadhar, K. (2012). *Commun Nonlinear Sci-Numer.simulat*, 17, 2447 – 2462.
[21] Stewartson, K., (1953). *Mathematical Proceedings of the Cambridge Philosophical Society*, 49, 333-341.
[22] Umar Khan, Ahmed, N., & Mohyud-Din, S.T. (2017).*Neural computing & applications*, 28(1), 37-46.
[23] Yahaya, S.D., Aziz, Z.A., Ishmail, Z., & Salah, F. (2018). *Australian Journal of Mechanical Engineering*, 16(3), 213-229.

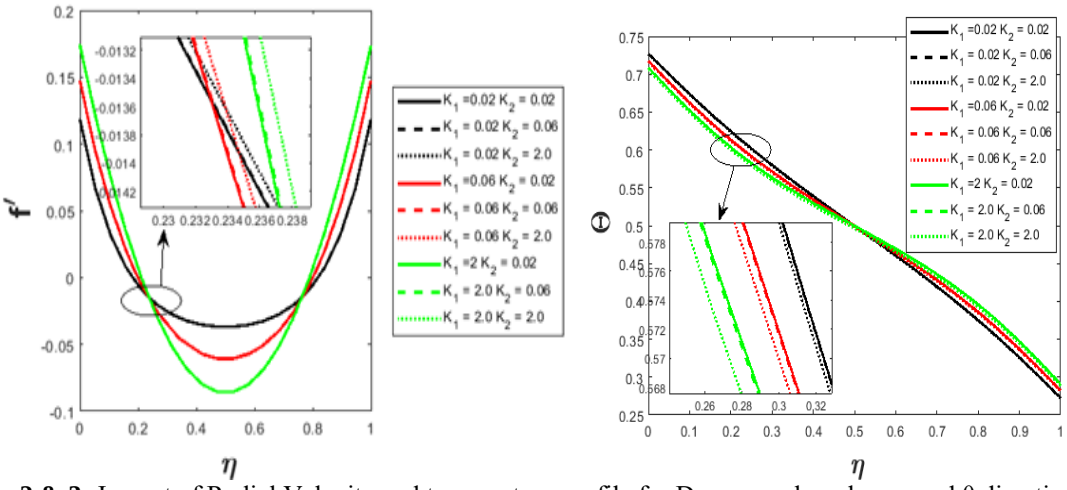

Figure 2 & 3: Impact of Radial Velocity and temperature profile for Darcy number along r and θ directions K_1 and K_2 respectively

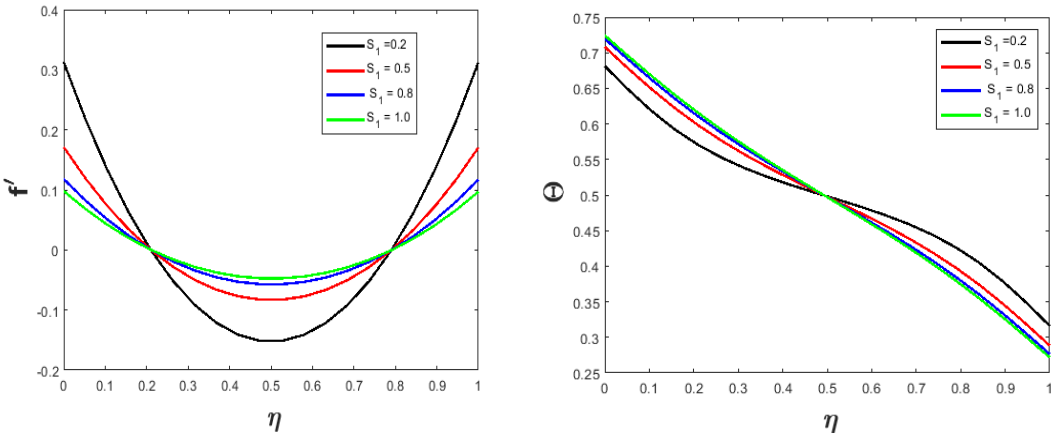

Figure 4 & 5: Impact of Radial Velocity and temperature profile for velocity slip parameter S_1 along r direction respectively

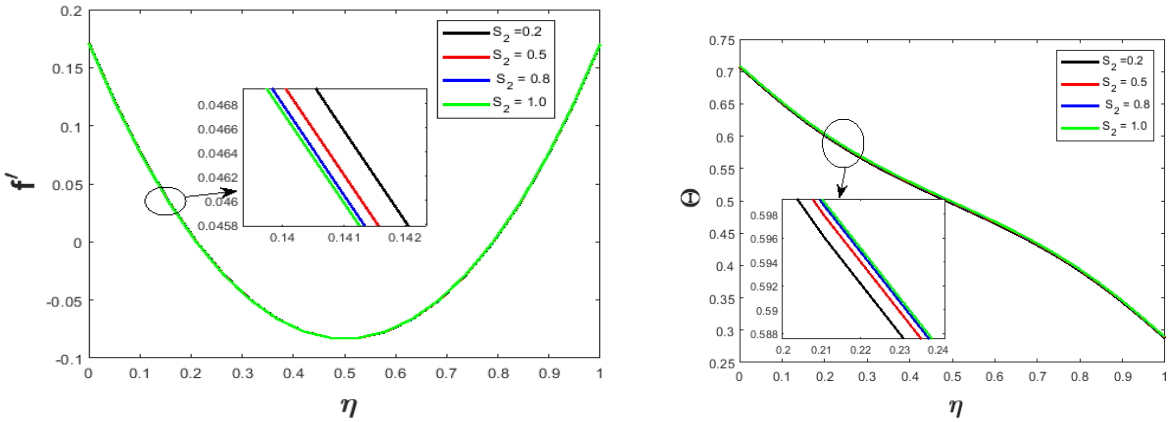

Figure 6 & 7: Impact of Radial Velocity and temperature profile for velocity slip parameter S_1 along θ direction respectively

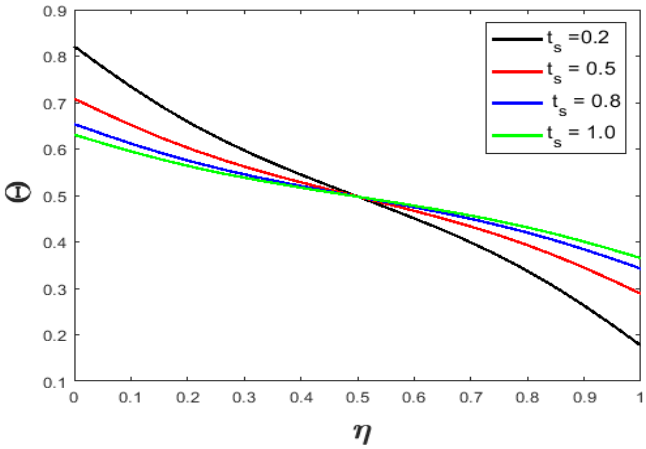

Figure 8: Impact of temperature profile for thermal slip parameter t_s

Table 2: Skin friction coefficient and Nusselt number values at lower and upper disks Re=10, S_1 = 0.5, S_2 = 0.5, Pr=6.23 and t_s = 0.5.

K_1	K_2	τ_1	τ_2	Nu_1	Nu_2
0.1	0.5	1.30330936	1.10239115	0.57309786	0.56852422
0.3		1.28412421	1.07992873	0.58156441	0.57539137
0.5		1.27973022	1.07478365	0.58354643	0.57691311
	0.1	1.60366438	1.20345599	0.58128270	0.57914191
	0.3	1.37323835	1.10542615	0.58276158	0.57769781
	0.6	1.25138061	1.06799629	0.58381379	0.57664248
	0.5	1.32081821	1.06155344	0.58446798	0.57597747

Table 3: Skin friction coefficient and Nusselt number values at lower and upper disks Re=10, Pr=6.23, K_1=0.5, K_2 = 0.5, Ω=0.5, R_1 = 0.7 and R_2 = 0.7

S_1	S_2	t_s	τ_1	τ_2	Nu_1	Nu_2
0.2	0.5	0.5	2.06583862	1.94685693	0.63738884	0.63223784
0.4			1.43941853	1.26107936	0.59601009	0.58973041
0.8			1.02386784	0.75124789	0.56051840	0.55320340
0.5	0.2		1.41996384	1.07085728	0.58624392	0.57429054
	0.4		1.31512488	1.07433233	0.58419374	0.57628455
	0.8		1.20927663	1.07394522	0.58233187	0.57809706
	0.5	0.2	1.27973022	1.07478365	0.89519926	0.88502331
		0.4	1.27973022	1.07478365	0.66015472	0.65265059
		0.8	1.27973023	1.07478365	0.43285366	0.42793331